

# Unconventional superconductivity in a strongly correlated band-insulator without doping

Anwesha Chattopadhyay<sup>1</sup>, H. R. Krishnamurthy<sup>2</sup>, Arti Garg<sup>1</sup>

<sup>1</sup> Condensed Matter Physics Division, Saha Institute of Nuclear Physics,  
HBNI, 1/AF Bidhannagar, Kolkata 700 064, India

<sup>2</sup> Centre for Condensed Matter Theory, Department of Physics,  
Indian Institute of Science, Bangalore 560 012, India

We present a novel route for attaining unconventional superconductivity (SC) in a strongly correlated system *without doping*. In a simple model of a *correlated band insulator* (BI) at *half-filling* we demonstrate, based on a generalization of the projected wavefunctions method, that SC emerges when e-e interactions and the bare band-gap are both much larger than the kinetic energy, provided the system has sufficient frustration against the magnetic order. As the interactions are tuned, SC appears sandwiched between the correlated BI followed by a paramagnetic metal on one side, and a ferrimagnetic metal, antiferromagnetic (AF) half-metal, and AF Mott insulator phases on the other side.

The discovery of unconventional superconductivity in a variety of materials, such as high  $T_c$  superconductivity in cuprates [1], iron pnictides and chalcogenides [2], in organic superconductors [3], heavy fermions [4] and very recently in magic angle twisted bilayer graphene [5, 6], has always ignited worldwide interest owing to their rich phenomenology, the theoretical challenges they pose, scientific implications and broad application potential. In almost all of these examples, superconductivity appears upon *chemically doping* a parent compound *away from commensurate filling* [1, 2, 5–8], though in some cases inducing charge fluctuations by changing pressure also leads to the superconducting phase [3, 8]. An important experimental fact is that chemical doping inevitably induces disorder, as is clearly the case in high  $T_c$  superconductors, which makes these materials very inhomogeneous [9–12]. It is a theoretical and experimental challenge to come up with new mechanisms and materials for *clean* high  $T_c$  superconductors.

Strong e-e correlations are crucial for unconventional superconductivity (SC). In most of the known unconventional superconductors [1–3, 5–8] the low temperature phase of the parent compound is either a strongly correlated antiferromagnetic (AF) Mott insulator where charge dynamics is completely frozen, or a AF spin-density-wave phase with at least moderately strong correlations. But the possibility of a SC phase in a *strongly correlated band-insulator* has been explored very little so far, either theoretically or experimentally.

In this work, we show how an AF spin-exchange mediated SC can be realized *without doping* in a simple model of a strongly correlated band insulator (BI), where the bare band gap ( $\Delta$ ) and the e-e interaction ( $U$ ) both dominate over the kinetic energy. As  $U$  is increased (but still remains of the order of  $\Delta$ ), the single particle excitation gap in the BI closes, resulting in a metallic phase. Upon further increasing  $U$ , SC develops by the formation of a coherent macroscopic quantum condensation of electron pairs, provided the metal has enough low energy quasi-particles and the system has enough frustration against the magnetic order. The SC features tightly bound short

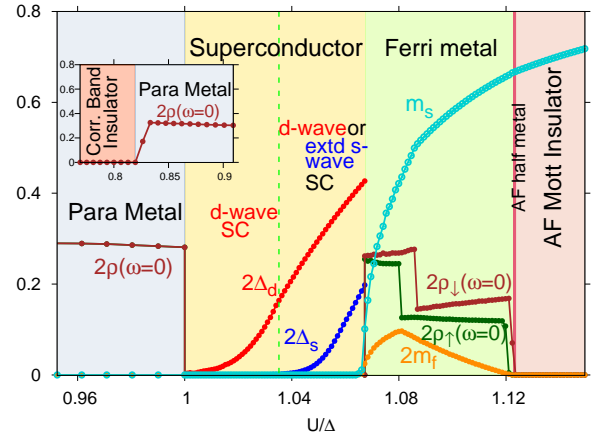


FIG. 1: Zero temperature phase diagram for the ionic Hubbard model (see text) on a square lattice with e-e interaction  $U = 10t$  and  $t' = 0.4t$  as a function of the interaction to bare band-gap ratio ( $U/\Delta$ ). For  $\Delta \gg U \gg t$ , the system is a correlated BI without any magnetic order. On increasing  $U/\Delta$ , first the gap in the single particle excitation spectrum closes, as shown by the non-zero single particle density of states at the Fermi energy  $\rho(\omega = 0)$ , resulting in a metallic phase. On further increasing  $U/\Delta$ , SC sets in and lasts over a significantly broad range ( $\Delta \in [9.3 : 10]t$ ) before ferrimagnetic order with non-zero staggered ( $m_s$ ) and uniform ( $m_f$ ) magnetization sets in via a first order transition. This is a Ferri metal phase with non-zero, spin asymmetric, spectral density at the Fermi-level:  $\rho_\uparrow(\omega = 0) \neq \rho_\downarrow(\omega = 0) > 0$ . As  $U/\Delta$  increases further,  $m_f \rightarrow 0$  whence the magnetic order becomes AF and an up-spin spectral gap opens up such that  $\rho_\uparrow(\omega = 0) = 0$  while the down-spin electrons are still conducting, resulting in a sliver of AF half-metal. Eventually the system becomes an AF Mott insulator as  $U/\Delta$  increases further.

coherence length Cooper pairs with a  $T_c$  well separated from the energy scale at which the pairing amplitude builds up. The phase diagram, whose section with all model parameters fixed except for  $U/\Delta$  is shown in Fig.1, presents a plethora of exoctic phases in the vicinity of a broad region of the SC phase.

Our starting point is a variant of the Hubbard model,

known as the *ionic* Hubbard model (IHM), where, on a bipartite lattice with sub-lattices A and B, a staggered ionic potential  $\Delta/2$  is present in addition to coulomb repulsion ( $U$ ):

$$\mathcal{H} = - \sum_{i,j,\sigma} (t_{ij} c_{i\sigma}^\dagger c_{j\sigma} + h.c.) - \mu \sum_i n_i - \frac{\Delta}{2} \sum_{i \in A} n_i + \frac{\Delta}{2} \sum_{i \in B} n_i + U \sum_i n_{i\uparrow} n_{i\downarrow} \quad (1)$$

The amplitude for electrons with spin  $\sigma$  to hop between sites  $i$  and  $j$  is  $t_{ij} = t$  for near-neighbours and  $t_{ij} = t'$  for second neighbours. The chemical potential  $\mu$  is chosen to fix the average occupancy at  $n = 1$  (half-filling). The staggered potential doubles the unit cell, and (for  $t' < \Delta/4$ ) induces a gap between the two electronic bands that result, making the system a BI for  $U = 0$ .

The parameter range of interest for this work is  $U \sim \Delta \gg t, t'$ , where a theoretical solution can be obtained based on a generalization of the projected wavefunctions method [13–19]. In this limit, at half-filling holons (doublons) are energetically expensive on the A (B) sites and can be projected out of the low energy Hilbert space. Consequently, though all hopping processes connecting the low and high energy sectors of the Hilbert space are eliminated, the system still has charge dynamics through first neighbor hopping processes such as  $|d_A h_B\rangle \Leftrightarrow |\uparrow_A \downarrow_B\rangle$  (with  $d$  representing a doublon and  $h$  a holon) and second neighbour hopping processes which allow doublons (holons) to hop on the A (B) sublattice [20].

The effective low energy Hamiltonian at half-filling,  $H_{eff}$ , is an extended  $t - t' - J - J'$  model acting on a projected Hilbert space:

$$\begin{aligned} H_{eff} = \mathcal{P} \left[ \left( -t \sum_{\langle ij \rangle, \sigma} c_{iA\sigma}^\dagger c_{jB\sigma} - t' \sum_{\langle\langle ij \rangle\rangle, \alpha, \sigma} c_{i\alpha\sigma}^\dagger c_{j\alpha\sigma} + h.c. \right) \right. \\ + J' \sum_{\langle\langle ij \rangle\rangle} \sum_{\alpha} S_{i\alpha} \cdot S_{j\alpha} - \frac{1}{4} (2 - n_{iA}) (2 - n_{jA}) - \frac{1}{4} n_{iB} n_{jB} \\ + J \sum_{\langle ij \rangle} \left( S_{iA} \cdot S_{jB} - (2 - n_{iA}) n_{jB} / 4 \right) - \mu \sum_i n_i \\ \left. + H_0 + H_d + H_{tr} + \dots \right] \mathcal{P} \quad (2) \end{aligned}$$

Here  $J = 2t^2/(U + \Delta)$  and  $J' = 4t'^2/U$ .  $H_0$  is the rescaled Hubbard interaction term in the projected Hilbert space and  $H_d$  ( $H_{tr}$ ) indicates other dimer (trimer) processes. We treat the projection constraint in  $H_{eff}$  using the generalised Gutzwiller approximation [18] and solve it using a renormalized Bogoliubov mean field theory. Gutzwiller approximations [15, 16, 18] of the sort we use have been well vetted against quantum Monte Carlo calculations [14, 19] and dynamical mean field theory [18]. Details of this *renormalized mean field theory*, Gutzwiller approximation and the various terms in  $H_{eff}$  are given in the Supplementary Material (SM) [21].

Our main findings are summarised in the phase diagram of Fig. 1, which shows a linear section (along the  $U/\Delta$  axis) of the full phase diagram in Fig. 2[e], for the IHM on a 2d square lattice at  $t' = 0.4t$ . The correlated

BI, stable for  $\Delta \gg U \gg t$ , is paramagnetic and adiabatically connected to the BI phase of the non-interacting IHM. As  $\Delta$  approaches  $U$ , the low energy hopping processes ( $|d_A h_B\rangle \Leftrightarrow |\uparrow_A \downarrow_B\rangle$ ) become more prominent, increasing charge-fluctuations such that the gap in the single particle excitation spectrum closes, leading to a paramagnetic metallic (PM) phase with finite single particle density of states (DOS)  $\rho(\omega = 0)$  at the Fermi energy, though for most of the parameter regime the PM phase is a compensated semi-metal with small Fermi pockets (Fig. 3 and following discussion) [22]. On further increasing  $U/\Delta$ , in the presence of sufficiently large  $t'$ , robust SC sets in for  $\Delta \sim U$  over a broad range of  $U/t$  (as shown in SM) due to the formation of coherent Cooper pairs of quasi-particles which live near the Fermi pockets, and survives for a sizeable range of  $\Delta$  ( $\in [9.3 : 10]t$ ). The pairing amplitudes  $\Delta_{d/s}$  for both the pairing symmetries we have studied, namely, the d-wave and the extended s-wave, increase monotonically with  $U/\Delta$  and drop to zero via a first order transition at the transition to the ferrimagnetic metal [27].

The ferrimagnetic metal (FM) phase is characterised by non-zero values of the staggered and uniform magnetizations  $m_{s,f} = (m_A \mp m_B)/2$  with  $m_{A/B}$  being the sublattice magnetizations, along with finite spin asymmetric DOS  $\rho_\sigma(\omega = 0)$  at the Fermi energy. With further increase in  $U/\Delta$  the FM evolves into an AF *half-metal* phase in which the system has only staggered magnetization (i.e.,  $m_f = 0$ ) and the single particle excitation spectrum for up-spin electrons is gapped while the down-spin electrons are still in a semi-metal phase. Eventually, for a large enough  $U/\Delta$ , both spin spectra become gapped - the system becomes an AF Mott insulator [31].

We next discuss the changes in the behavior of the system with increasing  $U/\Delta$  for varying values of  $t'$ , as depicted in Fig. 2. For  $t' = 0$ , the system shows a direct first order transition from an AF ordered phase to a correlated BI with a sliver of a half-metallic AF phase close to the AF transition point, consistent with most other theoretical work in this limit [32–35] barring one exception [36]. When  $t'$  is non-zero but small, due to the breaking of particle-hole symmetry as well as the frustration induced by the second neighbour spin-exchange coupling  $J'$ , the system first attains ferrimagnetic order for a range of  $U/\Delta$ , beyond which it has pure AF order as shown in panels (a,b) of Fig. 2. The magnetic transition occurs at increasingly larger values of  $U/\Delta$  with increasing  $t'$  (except for an initial decrease for small values of  $t'$ ), which helps in the development of a stable SC phase.

To stabilize the SC phase, a minimum threshold value of  $t'$  (which is a function of  $U$ ) is required, partly in order to frustrate the magnetic order as mentioned above, but more importantly to gain sufficient kinetic energy by intra-sublattice hopping of holons and doublons on their respective sublattices where they are energetically allowed. While a stable d-wave SC phase turns on for  $t' > 0.1t$  for  $U = 10t$ , as shown in Fig. 2, SC in the extended s-wave channel gets stabilized for much larger value of

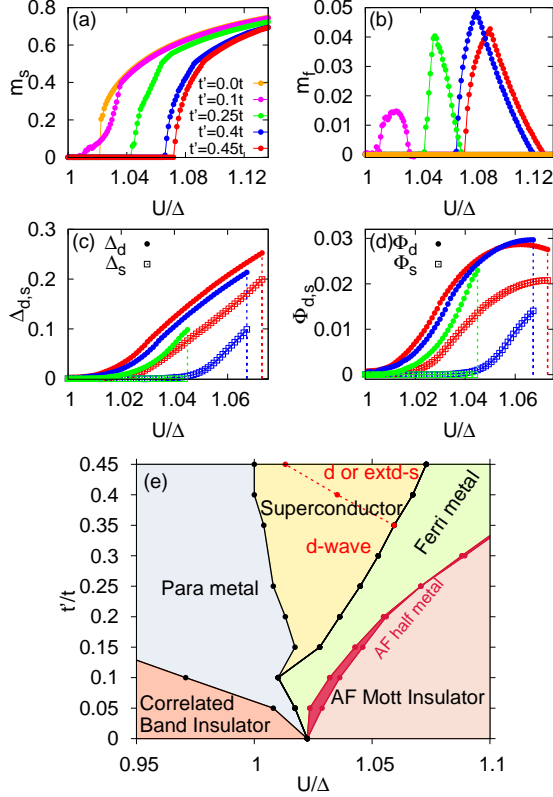


FIG. 2: Top panels show the staggered and uniform magnetization as functions of  $U/\Delta$  for several values of  $t'$  and  $U = 10t$ . With increasing  $t'$ , the magnetic transition point first decreases for  $t' \leq 0.12t$ , and then starts increasing again. The magnetic transition is of first order for  $t' = 0$  as well as for large values of  $t'$ , though for intermediate values of  $t'$  the magnetization tuns on continuously. Panel (c) shows the SC pairing amplitude  $\Delta_{d/s}$ , for the d-wave and extended s-wave pairing symmetry. With increasing  $t'$  the range in  $U/\Delta$  over which the SC is stable gets wider, and the amplitudes of both d-wave and extended s-wave pairings get enhanced. Panel (d) shows the SC order parameter  $\Phi_{d/s}$ , which also gives an estimate of the SC transition temperature,  $T_c$ . The bottom panel (e) shows the complete zero temperature phase diagram for  $U = 10t$  in the  $t'/t$ - $U/\Delta$  plane.

$t' > 0.35t$ . In an intermediate regime of  $U/\Delta$  and  $t'$ , states with both d-wave and extended s-wave symmetry are viable solutions with energies that are very close (See SM for details). As  $t'$  increases, the pairing amplitude increases and the range of  $U/\Delta$  over which the SC phase exists becomes broader for both the pairing symmetries studied [37].

The SC order parameter  $\Phi_{d/s}$  is defined in terms of the off-diagonal long-range order in the correlation function  $F_{\gamma_1\gamma_2}(\mathbf{r}_i - \mathbf{r}_j) = \langle B_{i\gamma_1}^\dagger B_{j\gamma_2} \rangle \rightarrow \Phi_{\gamma_1} \Phi_{\gamma_2}$  as  $|\mathbf{r}_i - \mathbf{r}_j| \rightarrow \infty$ , where  $B_{i\gamma}^\dagger$  creates a singlet on the bond  $(i, i + \gamma)$ . Fig. 2 shows the SC order parameter, which has been obtained after taking care of renormalization required in the projected wavefunction scheme (see SM). Since the SC order parameter for this system is much smaller than the strength of the pairing amplitude, with increase in

temperature the SC will be destroyed at  $T_c$  by the loss of coherence among the Cooper pairs, leaving behind a pseudo-gap phase with a soft gap in the single particle density of states due to the Cooper pairs which will exist even for  $T > T_c$ . Thus  $\Phi_{d/s}$  also provides an estimate of the SC transition temperature  $T_c$ . The maximum estimated  $T_c$  for  $U = 10t$  on a square lattice is approximately  $0.03t$  for the d-wave SC phase, which for a hopping amplitude comparable to that in cuprates ( $t \sim 0.4eV$ ) gives a  $T_c \sim 150K$ , and there is a considerable scope for enhancing  $T_c$  by tuning  $U/\Delta$  as well as  $t'$ .

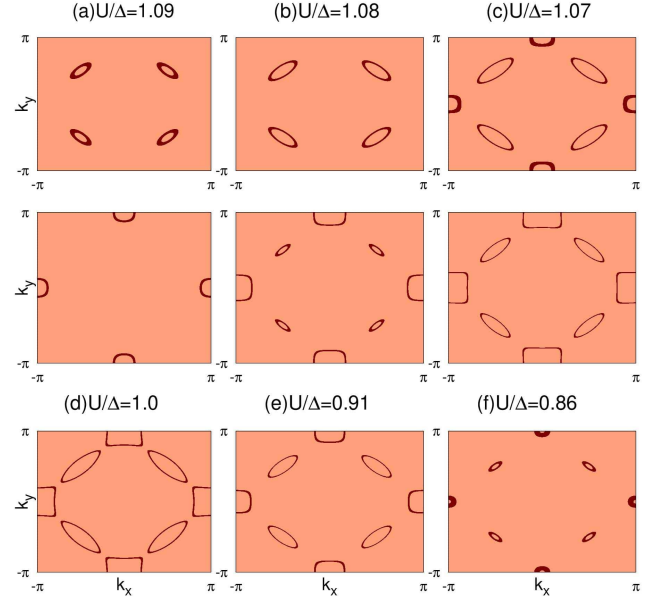


FIG. 3: The top two rows show the spin resolved low energy spectral functions  $A_\sigma(k, \omega \sim 0)$  (integrated over  $|\omega| \leq (0.01 - 0.02)t$  for a  $3000 \times 3000$  system) in the full BZ in the FM phase for  $t' = 0.35t$ ,  $U = 10t$ , with up-spin (down-spin) spectral functions shown in the first (second) row. At  $U/\Delta = 1.09$ , the up spin channel has electron pockets while the down spin channel has small hole pockets. As  $U/\Delta$  decreases, these Fermi pockets become bigger, the down (up) spin spectral function gets additional electron (hole) pockets. The last row shows  $A(k, \omega \sim 0)$  (same for up or down spins) for the PM phase. Moving towards the SC phase by increasing  $U/\Delta$ , Fermi pockets in the PM state go on expanding until they almost start touching each other, at which point the SC sets in by formation of Cooper pairs between electrons close to the Fermi energy.

A striking feature of the phase diagram in Fig. 2 is that, though the origin of SC in this model is due to the AF spin-exchange interactions, SC sets in only after the system has evolved to a PM or a FM phase. In order to understand the charge dynamics as the system approaches the SC phase, we have analysed the single particle spectral functions  $A_\sigma(k, \omega \sim 0)$  which can be directly measured in angle resolved photoemission spectroscopy (ARPES). Fig. 3 shows  $A_\sigma(k, \omega \sim 0)$ , non-zero values of which determine the energy contours on which low energy quasiparticles live in the Brillouin zone (BZ)

(see SM for details). Panels (a-c) show  $A_\sigma(k, w \sim 0)$  in the FM phase for which the up-spin channel has electron pockets around the points  $\mathbf{K} = (\pm\pi/2, \pm\pi/2)$  in the BZ and the down spin channel has small hole pockets around the points  $\mathbf{K}' = (\pm\pi, 0), (0, \pm\pi)$  (see SM for details), as shown in panel (a). As  $U/\Delta$  decreases within the FM phase, and approaches the SC phase, the electron pockets (hole-pockets) in the up-spin (down-spin) spectral function become bigger, and the down-spin channel gets additional electron pockets while the up-spin channel gets additional hole pockets, as shown in panel (c).

In the PM phase,  $A(k, w \sim 0)$  has spin symmetric electron pockets (around  $\mathbf{K}$ ) and hole pockets (around  $\mathbf{K}'$ ). As  $U/\Delta$  increases through the PM phase, these Fermi pockets slowly expand such that they almost touch each other before the system enters into the SC phase. Similar behaviour is seen with an increase of  $t'$  in the PM or the FM phases (see SM for details).

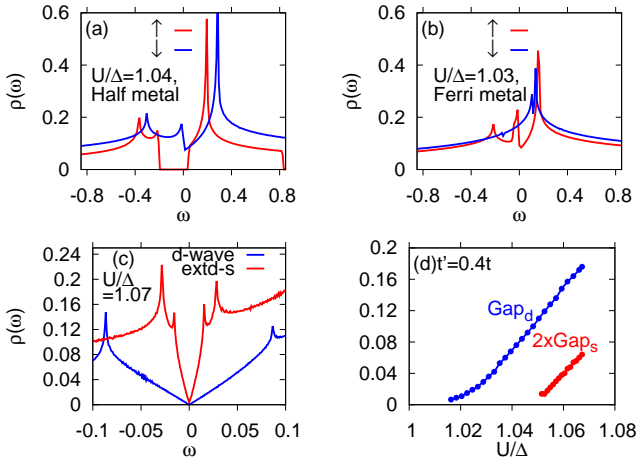


FIG. 4: Panels (a)-(b) show the spin resolved single particle density of states (DOS)  $\rho_\sigma(\omega)$  for  $t' = 0.15t$  and  $U = 10t$ . At  $U/\Delta \sim 1.04$ ,  $\rho_\downarrow(\omega = 0)$  is finite where as  $\rho_\uparrow(\omega = 0) = 0$  with a finite spectral gap, corresponding to the AF half-metal phase. At  $U/\Delta = 1.03$ , the DOS at the Fermi energy is finite in both the spin channels but  $\rho_\uparrow(\omega) \neq \rho_\downarrow(\omega)$  corresponding to the FM phase. Panel (c) shows  $\rho(\omega)$  for the d-wave and extd-s-wave SC phases for  $U = 10t$  and  $t' = 0.4t$ .  $\rho(\omega)$  shows a linear increase with  $|\omega|$  for  $\omega \sim 0$  for both the SC phases. Panel (d) shows the gap in the DOS, which is the peak to peak distance in  $\rho_\sigma(\omega)$ , for both the d-wave and the extended s-wave pairing symmetries.

Fig. 4. shows the spin-resolved DOS  $\rho_\sigma(\omega)$  vs  $\omega$  which provides additional evidence for the existence of various metallic phases as depicted in the phase diagram in Fig. 2. The para metal, ferri-metal and the AF half-metal phases are all compensated semi metals, which is reflected in the depletion in the DOS at the Fermi energy and is consistent with the small Fermi pockets shown in Fig. 3. We have also analysed the DOS in the SC phase. As shown in Fig. 4[c],  $\rho(\omega \sim 0) \sim |\omega|$  which is a signature of the gapless nodal excitations in the d-wave SC phase. Interestingly, even for the extended

s-wave SC phase  $\rho(\omega \sim 0) \sim |\omega|$  as the pairing takes place around the small Fermi pockets centered at the  $\mathbf{K}$  or  $\mathbf{K}'$  points in the BZ, where the pairing amplitude  $\Delta_s(k) = \Delta_s(\cos(k_x) + \cos(k_y))$  has nodes as well, resulting in gapless excitations. The gap, which is the peak to peak distance in the DOS, is much larger in the d-wave SC phase than in the extended s-wave phase, consistent with the former being the stable phase. Infact for the extended s-wave phase,  $\text{Gap}_s$  is only slightly larger than the SC order parameter  $\Phi_s$ , which indicates that the extended s-wave SC phase will have a narrower pseudogap phase above  $T_c$ , compared to the d-wave case.

The origin of unconventional SC in most of the materials known today [3, 5, 7, 8] can be understood in terms of the strongly correlated limit of the paradigmatic Hubbard model (single or multi band) but only upon doping the system away from half-filling [7, 8, 19, 38–40]. In the theoretical model we have studied here, SC appears even at half-filling, and therefore without the disorder that inevitably accompanies doping. A remarkable feature is that the SC phase in this model of a correlated BI is sandwiched between paramagnetic metallic and ferrimagnetic metallic phases, which makes the zero temperature phase diagram very different from that of the known unconventional SCs like high  $T_c$  cuprates [7] or the more recent magic angle twisted bilayer graphene [5]. We expect that the SC phase in this model has transition temperatures comparable to those of cuprates and that it also has a pseudogap phase like in cuprates.

The IHM has been realized for ultracold fermions on an optical honeycomb lattice [41], where the state-of-the-art engineering allows the parameters in the Hamiltonian to be tuned with great control. Hence it will be interesting and perhaps the easiest to explore our theoretical proposal in these systems. In the context of the recent developments in layered materials and heterostructures, it is possible to think of many scenarios where the IHM can be used as a minimal model, for example, graphene on h-BN substrate or bilayer graphene in the presence of a transverse electric field [42] which generates the staggered potential. The limit of strong correlation, crucial for realizing the SC phase, can be achieved in these materials by applying a strain or twist. Band insulating systems with two inequivalent strongly correlated atoms per unit cell, frustration in hopping and antiferromagnetic exchange, and lack of particle-hole symmetry, are likely tantalizing candidate materials as well. Our work suggests that the search for such novel materials where superconductivity can be realized at half filling with sufficiently high transition temperatures can perhaps emerge as an exciting, though challenging new research frontier in condensed matter physics.

A. G. and H. R. K gratefully thank the Science and Engineering Research Board of the Department of Science and Technology, India for financial support under grants No. CRG/2018/003269 and SB/DF/005/2017 respectively. A. C. acknowledges financial support by Department of Atomic Energy, Government of India.

- 
- [1] J. G. Bednorz, K. A. Müller, Z. Phys. B- Condensed Matter **64**, 189 (1986).
- [2] Y. Kamihara, T. Watanabe, M. Hirano, and H. Hosono, J. Am. Chem. Soc. **130**, 3296 (2008).
- [3] S. Lefebvre et.al., Phys. Rev. Lett. **85**, 5420 (2000).
- [4] M. Sigrist and K. Ueda, Rev. Mod. Phys. **63**, 239 (1991).
- [5] Y. Cao et. al, Nature **556**, 43 (2018).
- [6] E. Codecido et. al, Science Advances, **5**, no 9 (2019).
- [7] P. A. Lee, N. Nagaosa, and X. G. Wen, Rev. Mod. Phys. **78**, 17-85 (2006).
- [8] Q. Si, R. Yu, and E. Abrahams, Nature Rev. Mater. **1**, 16017 (2016).
- [9] S. H. Pan, J. P. O'Neal, R. L. Badzey, C. Chamon, H. Ding, J. R. Engelbrecht, Z. Wang, H. Eisaki, S. Uchida, A. K. Gupta, K.-W. Ng, E. W. Hudson, K. M. Lang, and J. C. Davis, Nature **413**, 282-285 (2001).
- [10] K. McElroy, J. Lee, J. A. Slezak, D. H. Lee, H. Eisaki, S. Uchida, and J. C. Davis, Science **309**, 1048-1052 (2005).
- [11] A. Garg, M. Randeria, and N. Trivedi, Nature Physics **4**, 762 (2008).
- [12] S. Tang, V. Dobrosavljevi, E. Miranda, Phys. Rev. B, **93**, 195109 (2016).
- [13] F. C. Zhang, C. Gros, T. M. Rice, and H. Shiba, Supercond. Sci. Tech. **1**, 36 (1988).
- [14] A. Paramekanti, M. Randeria, and N. Trivedi, Phys. Rev. Lett. **87**, 217002 (2001).
- [15] B. Edegger, C. Gros, V. N. Muthukumar, Adv. Phys. **56**, 927-1033 (2007).
- [16] M. Ogata, and A. Himeda, J. Phys. Soc. Jpn. **72**, 2 (2003).
- [17] W. H. Ko, C. P. Nave, and P. A. Lee, Phys. Rev. B, **76**, 245113 (2007).
- [18] A. Chattopadhyay, and A. Garg, Phys. Rev. B **97**, 245114 (2018).
- [19] P. W. Anderson, P. A. Lee, M. Randeria, T. M. Rice, N. Trivedi, and F. C. Zhang, J. Phys. Cond. Mat. **16**, R755-769 (2004).
- [20] Note that this is in contrast to the strongly correlated limit of the half-filled Hubbard model, where the kinetic energy gets fully projected out from the low energy Hilbert space, resulting in purely insulating phases.
- [21] The Supplemental Material contains technical details regarding the model and methods used in our calculations, as well as additional results complementing those presented in the main text.
- [22] This PM phase is adiabatically connected to the metallic phase observed for weak to intermediate strength of  $U/t$  as long as  $U \sim \Delta$  and the system is constrained to be paramagnetic, as shown in earlier work on the IHM using DMFT and other approaches [23–26]
- [23] A. Garg, H. R. Krishnamurthy, and M. Randeria, Phys. Rev. Lett. **97**, 046403 (2006).
- [24] N. Paris, K. Bouadim, F. Hebert, G. G. Batrouni, and R. T. Scalettar, Phys. Rev. Lett. **98**, 046403 (2007).
- [25] A. T. Hoang, J. Phys.: Cond. Matt. **22**(9), 095602 (2010).
- [26] L. Craco, P. Lombardo, R. Hayn, G. I. Japaridze, and E. Muller-Hartmann, Phys. Rev. B **78**, 075121 (2008).
- [27] Though there is a metastable state in which the SC phase coexists along with the ferrimagnetic order for a range of  $U/\Delta$  after the magnetic transition (see SM for details), due to the really tiny Zeeman splitting ( $\leq 0.035t$  for  $U = 10t$ ) produced by the small uniform magnetization  $m_f$  the possibility of a Fulde-Ferrel-Larkin-Ovchinnikov (FFLO) state seems unlikely [28–30].
- [28] P. Fulde, and R. A. Ferrell, Phys. Rev. **135**, A550 (1964).
- [29] A. I. Larkin, and Y. N. Ovchinnikov, Zh. Eksp. Teor. Fiz. **47**, 1136 (1964) [Sov. Phys. JETP **20**, 762 (1965)].
- [30] A. Datta, K. Yang, and A. Ghosal, Phys. Rev. B **100**, 035114 (2019).
- [31] Though we have studied the IHM on the simplest square lattice, a qualitatively similar phase diagram is expected on any bipartite lattice with changes involving appropriate symmetries, e.g.,  $d + id$  pairing symmetry on a honeycomb lattice.
- [32] A. Chattopadhyay, S. Bag, H. R. Krishnamurthy, and A. Garg, Phys. Rev. B **99**, 155127 (2019).
- [33] T. Watanabe, S. Ishihara, J. Phys. Soc. Jpn. **82**, 034704 (2013).
- [34] S. Bag, A. Garg, H. R. Krishnamurthy, Phys. Rev. B **91**, 235108 (2015).
- [35] S. S. Kancharla, and E. Dagotto, Phys. Rev. Lett. **98**, 016402 (2007).
- [36] A. Samanta and R. Sensarma, Phys. Rev. B **94**, 224517 (2016).
- [37] Though  $t'$  helps in the formation of the SC phase with pairing amplitudes living on the nearest neighbour bonds, there is no significant second neighbour pairing induced by  $J'$ .
- [38] P. W. Anderson, Science **235**, 1196-1198 (1987).
- [39] G. Kotliar, and J. Liu, Phys. Rev. B **38**, 5142-5145 (1988).
- [40] A. V. Mallik, G. K. Gupta, V. B. Shenoy, and H. R. Krishnamurthy, Phys. Rev. Lett. **124**, 147002 (2020).
- [41] M. Messer et. al, Phys. Rev. Lett. **115**, 115303 (2015).
- [42] E. V. Castro et. al, Phys. Rev. Lett. **99**, 216802 (2007).